Spread-Response Precoding for Communication over Fading Channels

Gregory W. Wornell, *Member, IEEE*

Abstract—**Interleaving is an important technique for improving the effectiveness of traditional error-correcting codes in data transmission systems that exhibit multipath fading. Such channels often arise in mobile wireless communications. We present an alternative to interleaving for such systems, which we term "spread-response precoding." From the perspective of the coded symbol stream, spread-response precoding effectively transforms an arbitrary Rayleigh fading channel into a nonfading, simple white marginally Gaussian noise channel. Furthermore, spread-response precoding requires no additional power or bandwidth, and is attractive in terms of computational complexity, robustness, and delay considerations.**

Index Terms—**Wireless communication, Rayleigh fading channels, diversity techniques, precoding, interleaving, smearing.**

I. Introduction

THE need to reliably transmit analog and digital data over channels subject to fading arises in a wide range of applications including mobile radio and personal wireless systems, and audio and television broadcasting. Generally, the fading characteristics of the channel, which are a function of both the nature of the transmission media and the relative motions of the transmitter and receiver lead to variations in the quality of channel both in time and in frequency.

Diversity techniques are widely used in communication systems to compensate for these variations [1], [2]. These range from simple multiple transmission strategies in time, frequency, and space, to more sophisticated diversity techniques based on the use of coding. In such scenarios, coding is used to combat both the effects of fading and the effects of stationary additive noise.

In order for coding to be effective against fading in particular, it is generally necessary to combine coding with interleaving, a simple but nevertheless useful form of precoding. The purpose of interleaving is to scramble the coded data stream so that fading channel effectively seen by this stream is uncorrelated from time-sample to time-sample. This substantially reduces the coding complexity required to achieve a given level of fidelity, allowing shorter lengths in the case of block codes, or fewer states in the case of convolutional codes.

In this paper, we develop an attractive alternative to interleaving which we term "spread-response precoding." With spread-response precoding, the fading channel as seen by the coded data stream is effectively transformed into a simple additive white noise channel. As a result, when combined with coding techniques such as trellis-coded modulation, the precoding stage combats any fading effects, while the coding stage combats the remaining additive noise. This partitioning appears to be rather attractive in terms of system complexity considerations. Indeed, spread-response precoding, in requiring comparatively simple linear signal processing at the transmitter and receiver, is significantly less demanding computationally than error-correcting coding and decoding algorithms. Moreover, precoding constitutes a diversity strategy that incurs no additional cost in terms of bandwidth or average power, and is competitive with traditional approaches in terms of robustness and delay considerations.

While it has generally been understood that interleaving is not the most efficient of precoding strategies (see, e.g., [3]), the literature has offered surprisingly few alternatives. Perhaps the work closest in spirit to the ideas presented here is that of Wittneben [4], although in that work precoding is developed for use in conjunction with interleaving rather than as an alternative to interleaving. Nevertheless, Wittneben's paper was among the first to explore some of the key ideas, and contains a number of important insights on the topic.

In this paper we restrict our attention to single-user systems, or equivalently, multiuser systems employing frequency-division multiplexing. However, we note in advance that powerful multiuser extensions of these ideas can be developed and lead to efficient new classes of code-division multiple-access (CDMA) systems; these are explored in detail in the companion paper [5].

The paper is organized as follows. In Section II, we outline the Rayleigh fading channel model we consider. In Section III, we develop the transmitter portion of the system, while in Section IV, we turn our attention to the receiver portion of the system, developing optimum designs. In Section V, we explore aspects of the performance of systems using precoding, including theoretical capacity and attainable bit error rate calculations. In Section VI, we discuss precoder design and implementation issues, and develop results on achievable performance with practical precoders. Finally, Section VII contains some concluding remarks.

Manuscript received April 26, 1994; revised October 2, 1995. This work was supported in large part by AT&T Bell Laboratories as well as by the Advanced Research Projects Agency monitored by ONR under Contract N00014-93-1-0686 and the Office of Naval Research under Grant N0014-95-1-0834. This work was performed while the author was on leave at AT&T Bell Laboratories, Murray Hill, NJ, during the 1992–1993 academic year. The material in this paper was presented in part at the IEEE International Symposium on Information Theory, Whistler, BC, Canada, Sept. 1995.

The author is with the Department of Electrical Engineering and Computer Science and the Research Laboratory of Electronics, Massachusetts Institute of Technology, Cambridge, MA USA.

Publisher Item Identifier S 0018-9448(96)01183-2.

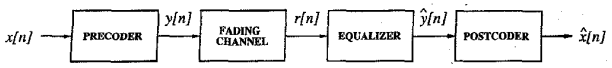

Fig. 1. Precoding system.

II. System Model

Fig. 1 depicts a block diagram of the overall system we consider. In this figure, $x[n]$ is the complex-valued M-ary symbol sequence representing the coded bit stream, and $y[n]$ is the precoded symbol stream to be transmitted. The transmitted data $y[n]$ are corrupted by complex-valued fading and additive noise, producing $r[n]$ at the receiver. The received data are first processed by an equalizer to produce $\hat{y}[n]$, then by a postcoder to produce $\hat{x}[n]$. Finally, a decoder (not shown) processes $\hat{x}[n]$ to produce an estimate of the original bit stream.

The channel in Fig. 1 is the equivalent discrete-time baseband model of a fairly general stationary Rayleigh fading channel with uncorrelated scattering and bandwidth $\mathcal{W}_0$. The channel consists of two components, a linear time-varying filter which captures the effects of multipath fading due to multiple scatters in the transmission medium, and an additive noise term representing both receiver noise and, more significantly, co-channel interference.

More specifically, the response of the channel to an input sequence $y[n]$ is given by

$$r[n] = \sum_k a[n;k]\, y[n-k] + w[n] \tag{1}$$

where $w[n]$ is a zero-mean complex stationary white Gaussian sequence with variance

$$E\left[|w[n]|^2\right] = \mathcal{N}_0\mathcal{W}_0$$

and $a[n;k]$, the response of the channel at time n to a unit-sample at time $n-k$, is a complex Gaussian fading process. For fixed values of k, the $a[n;k]$ are zero-mean complex-valued jointly stationary, Gaussian sequences. Furthermore, uncorrelated scattering implies sequences corresponding to distinct values of k are statistically independent. Hence

$$E[a[n;k]\, a^*[n-m;l]] = R_a[m;k]\, \delta[k-l]$$

where $\delta[n]$ is the unit-sample, i.e.

$$\delta[n] \triangleq \begin{cases} 1, & n=0 \\ 0, & \text{otherwise} \end{cases}. \tag{2}$$

With uncorrelated scattering, the time-variant channel frequency response[1]

$$A(\omega;n) = \sum_k a[n;k]\, e^{-j\omega k} \tag{3}$$

is then stationary in both n and ω and satisfies

$$E[A(\omega;n)] = 0 \tag{4a}$$

$$E\left[|A(\omega;n)|^2\right] = \sigma_a^2. \tag{4b}$$

[1] We adopt the useful convention of using parentheses $(\cdot)$ to denote continuous-valued arguments and brackets $[\cdot]$ to denote discrete-valued arguments. For functions of two arguments where the first is continuous and the second is discrete (as in the case of time-variant frequency responses) we use the convenient mixed notation $(\cdot;\cdot]$. The notation $[\cdot;\cdot)$ is used in a similar manner.

Both $w[n]$ and $a[n;k]$ are assumed to be statistically independent of the input to the channel.

Finally, we assume that while the transmitter does not have access to the fading channel kernel $a[n;k]$ or its statistics, these parameters are known, or more typically, can be reliably measured at the receiver.

III. Spread-Response Precoding

In this section, we consider, the transmitter portion of the system in Fig. 1. We begin by observing that although the detailed characteristics of a fading channel fluctuate from time sample to time sample, the performance of communication systems using such channels is generally dictated by the *average* characteristics of that channel over time. Certainly most capacity estimates for such channels involve averaging of this type; see, e.g., [6] and the references therein. As a consequence, an efficient communication strategy for such channels would, in some sense, "spread" the transmission of each symbol over a large number of time samples.

Conveniently, spreading of this type can be achieved through simple linear time-invariant (LTI) filtering of the coded symbol stream—a form of precoding. Specifically, denoting the unit-sample response of the precoding filter by $h[n]$, the transmitted sequence is[2] (cf. Fig. 1)

$$y[n] = x[n] * h[n] = \sum_k x[k]\, h[n-k]. \tag{5}$$

For convenience, we restrict our attention to the case in which $h[n]$ is a real-valued sequence.

It is also highly desirable for the precoding to be lossless, in which case $y[n]$ constitutes an orthonormal transformation of the data symbols $x[n]$. Lossless LTI filters satisfy the time-domain constraint

$$\sum_n h[n-k]\, h[n-l] = \delta[k-l]. \tag{6}$$

In the frequency domain, the condition (6) corresponds to

$$|H(\omega)|^2 = 1 \tag{7}$$

and, for this reason, lossless filters are frequently referred to as *allpass* filters in the signal processing literature [7]. An important property of such filters which follows immediately from (6) is that

$$h^{-1}[n] = h[-n].$$

Accordingly, we may conveniently and stably recompute $x[n]$ from $y[n]$ according to

$$x[n] = y[n] * h[-n] = \sum_k y[k]\, h[k-n]. \tag{8}$$

From a practical standpoint, it is necessary to restrict our attention to finite impulse response (FIR) precoders. However, as is well known, the only lossless FIR filters are the shifted unit-samples, i.e., $h[n] = \delta[n-k]$ for arbitrary k. Nevertheless, many infinite impulse response (IIR) lossless

[2] We use operator $*$ to denote convolution, and the superscript * to denote complex conjugation.

filters have strongly localized temporal support and can be truncated without significantly altering their characteristics. More generally, there are a wide variety of FIR filters that closely approximate the losslessness condition (6).

To make this notion of approximation more precise, consider the class of LTI filters $h[n]$ with unit-energy, i.e.

$$\sum_n h^2[n] = 1 \tag{9}$$

and let

$$\Phi_h[n] = h[n] * h[-n] = \sum_k h[k]\, h[k-n]$$

denote the autocorrelation function. Then, since the autocorrelation of a perfectly lossless filter is the unit-sample, a useful measure of the deviation from losslessness is the reciprocal of the total sidelobe energy in the autocorrelation function. Specifically, we define the following convenient losslessness merit factor $\mathcal{L}_h$ for a unit-energy filter $h[n]$:

$$\mathcal{L}_h = \left(\sum_n \left(\Phi_h[n] - \delta[n] \right)^2 \right)^{-1} = \left(2 \sum_{n=1}^{\infty} \Phi_h^2[n] \right)^{-1} \tag{10}$$

with large $\mathcal{L}_h$ corresponding to filters that are nearly lossless. Specifically, we have $0 < \mathcal{L}_h \leq \infty$ with the right-hand equality if and only if the filter is perfectly lossless. This merit factor is identical to that introduced by Golay to evaluate the quality of low autocorrelation binary sequences [8].

While losslessness is an important attribute of a precoding filter, a second important attribute is their effectiveness in spreading the transmission of each symbol over a large number of time samples. This is achieved when the precoder's unit-sample response energy is widely dispersed in time, or equivalently, when the precoding system has strong partial response characteristics. Indeed, one can interpret spread-response precoding as a form of partial-response precoding, although the objectives of traditional partial-response precoding are markedly different.

A useful measure of dispersion for an arbitrary unit-energy filter $h[n]$ in the context of this work is given by

$$\mathcal{D}_h = \left(\sum_n h^4[n] \right)^{-1} \tag{11}$$

with large $\mathcal{D}_h$ corresponding to good spreading characteristics. Using (9), it follows that for unit-energy filters

$$\mathcal{D}_h \geq 1 \tag{12}$$

with equality when $h[n] = \delta[n]$. However, for FIR filters of length N with unit-energy, (9) also implies that

$$\mathcal{D}_h \leq N$$

with equality precisely when

$$|h[n]| = 1/\sqrt{N}, \quad \text{all } 0 \leq n \leq N-1 \, .$$

Consequently, for FIR precoders maximum dispersion (i.e., $\mathcal{D}_h = N$) is obtained when $h[n]$ is an antipodal (binary) sequence. Conveniently, binary sequences are also highly attractive in terms of both computational efficiency and numerical sensitivity.

While both good losslessness and spreading characteristics are desirable in design of FIR precoders, they are competing objectives. Based on the preceding discussion, at one extreme the precoder $h[n] = \delta[n]$ corresponds to the best possible $\mathcal{L}_h$ but the worst possible $\mathcal{D}_h$. At the opposite extreme, precoders with binary-valued unit-sample responses provide the best possible $\mathcal{D}_h$ for a given length constraint, but poor values of $\mathcal{L}_h$. Indeed, a conjecture of Golay [9] based on an ergodicity postulate suggests that for such binary sequences

$$\max_h \mathcal{L}_h \to 12.3247\cdots \quad \text{as } N \to \infty \, .$$

Consequently, as we will discuss later, for a fixed filter length prescribed by external delay constraints imposed on the overall system, the precoder design process requires a compromise between the two components.

As an aside, it is useful to note that the need for compromise can be avoided by relaxing the requirement that the precoder be linear and strictly time-invariant. In particular, if the broader class of linear periodically time-varying (LPTV) precoders are considered, then FIR systems can be readily contructed so as to be both lossless and maximally dispersive (i.e., have binary-valued unit-sample responses). Such generalizations are explored in detail in the companion paper [5].

When spread-response precoding is used in a system, the transmitted data have some rather special asymptotic characteristics. First, we note that with lossless precoding we get, via (7), that $y[n]$ will have same (average) power spectrum as the original coded data $x[n]$, i.e.

$$S_y(\omega) = S_x(\omega).$$

In particular, when $x[n]$ is a sequence of statistically independent complex-valued symbols each with energy $\mathcal{E}_s$, then $y[n]$ is a complex wide-sense-stationary white sequence with variance $\mathcal{E}_s$. In addition, it can be shown that in the limit of infinite dispersion ($\mathcal{D}_h \to \infty$) the transmitted stream is marginally Gaussian, i.e., that each transmitted sample $y[n]$ has a Gaussian distribution. This follows from a Central Limit Theorem argument: using (5) we see each $y[n]$ is the balanced sum of a large number of independent random variables. From the point of view of transmission security and capacity considerations, such characteristics are rather appealing. However, we should also note that from the point of view of peak-to-average power and receiver synchronization requirements, these characteristics present important practical challenges in terms of system design. However, such considerations are beyond the scope of the present paper.

IV. System Characteristics and Receiver Design

In this section, we turn our attention to the receiver in Fig. 1. We begin by noting that the receiver for decoding the bit stream can be partitioned into two stages. The first is the equalization stage, which, as depicted in Fig. 1 and, without loss of generality, can be described as the cascade of an equalizer and postcoder. The second is the decoding stage (not shown in Fig. 1) that typically consists of some

form of Maximum-Likelihood (ML) sequence detection. As will become apparent, when no coding is employed, simple symbol-by-symbol detection generally suffices at the decoder. However, in the sequel we restrict our attention to the equalization and postcoding stages.

In general, the equalizer, which compensates for the fading, is a linear time-varying filter whose kernel is $b[n;k]$, so that

$$\hat{y}[n] = \sum_k b[n;k]\, r[n-k].$$

Typically, this kernel is a function of the fading channel kernel $a[n;k]$ and the noise statistics, both of which are assumed to be available at the receiver.

In turn, the postcoder inverts the transformation of input symbols that takes place during precoding, and is simply a linear filter whose unit-sample response is (cf. (8)) a time-reversed version of the lossless precoding filter $h[n]$, i.e.

$$\hat{x}[n] = h[-n] * \hat{y}[n]. \tag{13}$$

The overall system consisting of the channel with precoding, equalization, and postcoding, will be referred to as the "composite channel." In the remainder of this section we first derive the key properties of this composite channel, then optimize them through judicious choice of the equalizer parameters.

Our main result is that subject to only relatively mild ergodicity constraints on the channel, the use of lossless precoding with a large dispersion factor leads asymptotically to an additive white noise composite channel that is free of fading. In order to make our result precise, we first define a sufficiently realistic class of ergodic kernels for our purposes, which we term "admissibly ergodic."

Definition 1: Let $f[n;k]$ be the kernel of a linear system, and define

$$\tilde{f}[n;k] = f[n;k] - E[f[n;k]]. \tag{14}$$

Furthermore, let

$$d[n;k] = \sum_l \tilde{f}[n;l]\, \tilde{f}^*[n-k;l-k] \tag{15}$$

and define

$$\tilde{d}[n;k] = d[n;k] - E[d[n;k]]. \tag{16}$$

Then $f[n;k]$ is an *admissibly ergodic* kernel if the following conditions are satisfied:

$$E[f[n;k]] = \mu\,\delta[k] \quad \text{for every } k,n \tag{17a}$$

$$E\left[\tilde{f}[n;k]\,\tilde{f}^*[n-m;l]\right] = R[m;k]\,\delta[k-l] \quad \text{for every } k,l,m,n \tag{17b}$$

$$E\left[\tilde{d}[n;k]\,\tilde{d}^*[n-m;l]\right] = T[m;k,l] \quad \text{for every } k,l,n,m \tag{17c}$$

$$S_R = \sum_k \sum_n |R[n;k]| < \infty \tag{17d}$$

$$S_T = \sum_{k,l} \sum_m |T[m;k,l]| < \infty. \tag{17e}$$

Before proceeding, we adopt some nomenclature. It will be convenient to view a generic linear kernel such as $f[n;k]$ as a collection of sequences in n indexed by k. Hence, when we refer to "the sequence $f[n;k]$" we specifically mean the sequence in n corresponding to a fixed (but generally arbitrary) value of k. From this viewpoint, the conditions in Definition 1 are straightforward to interpret. Conditions (17a)–(17c) are essentially stationarity constraints. They ensure, specifically, that the kernel sequences $f[n;k]$ and the correlation sequences $d[n;k]$ are each jointly wide-sense-stationary. The condition (17b) also ensures that sequences $f[n;k]$ corresponding to distinct values of k are uncorrelated. Finally, conditions (17d) and (17e) in effect ensure that linear combinations of the kernel sequences $f[n;k]$ are mean- and correlation-ergodic.

Equivalently, the conditions in Definition 1 can be interpreted in terms of stationarity and ergodicity constraints on the time-variant system frequency response

$$F(\omega;n) = \sum_k f[n;k]\, e^{-j\omega k}. \tag{18}$$

We note, in particular, that (17a) and (17b) imply that $F(\omega;n]$ is wide-sense-stationary in both n and ω and satisfies

$$E[F(\omega;n]] = \mu. \tag{19}$$

Furthermore, with

$$\tilde{F}(\omega;n] = F(\omega;n] - E[F(\omega;n]]$$

we have

$$E\left[\tilde{F}(\theta;n]\,\tilde{F}^*(\theta-\omega;n-m]\right] = \Psi(\omega;m] \tag{20}$$

where $\Psi(\omega;m]$ is the spaced-frequency spaced-time correlation function of the system and satisfies

$$\Psi(\omega;m] = \sum_k R[m;k]\, e^{-j\omega k}. \tag{21}$$

The multipath intensity profile or delay power spectrum of the system is therefore given by

$$\sigma_k^2 = R[0;k] = \operatorname{var} f[n;k] \tag{22}$$

and the total power is given by

$$\sigma^2 \triangleq \operatorname{var}[F(\omega;n]] = \Psi(0;0] = \sum_k \sigma_k^2. \tag{23}$$

We can now present our main theorem concerning the composite system depicted in Fig. 1. A proof is presented in Appendix I.

Theorem 1: Let $x[n]$ be a sequence of zero-mean, uncorrelated symbols, each with energy $\mathcal{E}_s$; let $a[n;k]$ and $w[n]$ be as defined in (1); and let $c[n;k]$ denote the kernel of the composite linear system formed by cascading the channel corresponding to kernel $a[n;k]$ with the equalizer corresponding to kernel $b[n;k]$, i.e.

$$c[n;k] = \sum_l b[n;l]\, a[n-l;k-l]. \tag{24}$$

Finally, suppose $c[n;k]$ and $b[n;k]$ are both admissibly ergodic kernels in the sense of Definition 1. Then, as $\mathcal{D}_h \to \infty$, we

have,[3] for each n

$$\hat{x}[n] \xrightarrow{\text{m.s.}} \mu_c\, x[n] + v[n] \tag{25}$$

where $v[n]$ is a complex-valued, marginally Gaussian, zero-mean white-noise sequence, uncorrelated with the input symbol sequence $x[n]$ and having variance

$$\operatorname{var} v[n] = \mathcal{E}_s\sigma_c^2 + \mathcal{N}_0\mathcal{W}_0(\sigma_b^2 + |\mu_b|^2). \tag{26}$$

Theorem 1 asserts that the use of sufficient precoding transforms the channel "seen" by the coded symbol stream from a fading channel into a marginally Gaussian white-noise channel. In particular, and as will become more apparent, the intersymbol interference usually generated by fading is transformed into a comparatively more benign form of additive white interference. As a result, the characteristics of the composite channel depend only on the statistics of the fading channel parameters $a[n;k]$ and $w[n]$ but *not* on the values of the parameters themselves. Not surprisingly, this is a natural consequence of the time averaging induced by precoding being applied to an ergodic fading process.

A few additional remarks regarding Theorem 1 are appropriate. First, as can be readily verified from the proof in Appendix I, Theorem 1 is true even when the kernel $a[n;k]$ and receiver noise $w[n]$ are not Gaussian. This observation is important for robustness, since these processes are at most approximately Gaussian in practice.

As a second comment, we also point out that the assumption of an uncorrelated symbol stream at the input to the precoder is a reasonable one, even when this input represents the output of a traditional coder. For example, when typical trellis codes are used with random bit streams, the output is generally a white symbol stream [10]. In addition, the use of random codes produces asymptotically white symbol streams.

Third, we emphasize that $v[n]$ in Theorem 1 is a marginally Gaussian process. Specifically, this means that $v[n]$ is a sequence of uncorrelated random variables each having a Gaussian distribution, but that the random variables are not necessarily jointly Gaussian. Hence, $v[n]$ is not necessarily a Gaussian random process, and, as a result, there may exist at least some statistical dependence among the noise samples. However, we shall assume that, in practice, $v[n]$ is an at least approximately Gaussian process, so that the statistical dependency among samples is negligible.

The noise $v[n]$ has other special characteristics as well. As is apparent from (26), the noise consists of the sum of two uncorrelated components. The first component has power $\mathcal{N}_0\mathcal{W}_0(\sigma_b^2 + |\mu_b|^2)$ and is due to the noise in the original fading channel. The second component has power $\mathcal{E}_s\sigma_c^2$ and is inherently generated in the precoding process. The existence of this second noise component means that boosting the transmitter power in the system also leads to an increase in noise power in the composite channel. For this reason, we shall find that the familiar matched-filter equalizer [11] is not best suited for use with precoding.

[3] We use the notation $\xrightarrow{\text{m.s.}}$ to denote, specifically, convergence in the mean-square sense.

Finally, we point out that although Theorem 1 establishes only an asymptotic result valid for perfectly lossless precoding with infinite dispersion (implying, for example, infinite delay), the asymptotic behavior can be approximated arbitrarily closely with realizable precoders. A discussion of the design and properties of finite-delay precoders is deferred to Section VI.

Let us now consider the design of the equalizer. We begin by observing that Theorem 1 implicitly imposes certain constraints on the equalizer kernel $b[n;k]$ in order that the equivalent channel model structure is attained asymptotically. These constraints are, from a practical standpoint relatively mild. Specifically, it suffices that $b[n;k]$ be chosen so that both $b[n;k]$ and the cascade of $a[n;k]$ with $b[n;k]$ (i.e., (24)), are admissibly ergodic. For convenience, let us refer to kernels $b[n;k]$ with this property as *admissible* equalizers.

Among the class of admissible equalizers, some yield better composite channels than others. One useful measure of the quality of the composite channel is the signal-to-noise ratio (SNR). Certainly when $v[n]$ is Gaussian then both the theoretical capacity and achievable bit error rates increase monotonically with the channel SNR. Consequently, a useful criterion for equalizer design is to select among the admissible equalizers that yielding the largest SNR in the composite channel. Conveniently, when $b[n;k]$ is an admissible equalizer, the SNR in the composite channel follows directly from Theorem 1 as

$$\gamma(b) = \frac{|\mu_c|^2}{\sigma_c^2 + \xi_0\,(\sigma_b^2 + |\mu_b|^2)} \tag{27}$$

where

$$\xi_0 = \mathcal{N}_0\mathcal{W}_0/\mathcal{E}_s. \tag{28}$$

In Sections IV-A and IV-B, we proceed to derive these optimum equalizers in the two cases of perhaps greatest interest in practice, corresponding to frequency-nonselective fading and frequency-selective slow fading, respectively.

A. Frequency-Nonselective Fading

In this section, we restrict our attention to the Rayleigh fading channel model of (1) with

$$a[n;k] = a[n]\,\delta[k].$$

in which case, as is straightforward to show, the admissible equalizers are also of the form

$$b[n;k] = b[n]\,\delta[k].$$

Accordingly, we may rewrite (27) in this scenario as

$$\gamma(b) = \frac{|E[ab]|^2}{\operatorname{var}[ab] + \xi_0 E[|b|^2]} \tag{29}$$

where ξ_0 is as defined in (28) and where we have omitted a specification of the time-sample n due to stationarity.

To derive the optimum equalizer, we begin by rewriting (29) as

$$\gamma(b) = \frac{1}{1/\varphi(b) - 1} \tag{30}$$

where

$$\varphi(b) = \frac{|E[ab]|^2}{E[(|a|^2 + \xi_0)|b|^2]} \tag{31}$$

and where we have exploited the identity

$$\text{var}\,[ab] = E\big[|ab|^2\big] - |E[ab]|^2.$$

Then, by the Schwarz inequality we have

$$\begin{aligned} |E[ab]|^2 &= \left| E\left[\frac{a}{\sqrt{|a|^2 + \xi_0}} \cdot b\sqrt{|a|^2 + \xi_0} \right] \right|^2 \\ &\le E\left[\frac{|a|^2}{|a|^2 + \xi_0} \right] E\big[(|a|^2 + \xi_0)|b|^2\big] \end{aligned}$$

with equality if and only if

$$b \propto \frac{a^*}{|a|^2 + \xi_0}.$$

Hence, (31), and, in turn, (29) are maximized when

$$b[n] \propto \frac{a^*[n]}{|a[n]|^2 + \xi_0} \tag{32}$$

where the (complex) constant of proportionality is arbitrary.

Not surprisingly, the optimum equalizer is specified only to within an arbitrary gain factor, since such factors do not affect the resulting SNR. In addition, it is interesting to note (and can be readily verified) that the equalizer yielding optimum SNR in the composite channel, i.e., (32), also corresponds, when suitably normalized, to a minimum mean-square-error linear equalizer for the fading channel. Specifically, $\hat{y}[n]$ and, in turn, $\hat{x}[n]$ are minimum mean-square-error linear estimates of $y[n]$ and $x[n]$, respectively. Although he did not establish its optimality, it was Wittneben [4] in his preliminary work on precoding for the nonselective fading channel with interleaving who first suggested that a minimum mean-square-error-type equalizer was well-suited to this scenario.

B. Frequency-Selective Fading

In this section, we consider the more general channel model (1) for which the fading is, in general, frequency-selective. This scenario generally arises when larger transmission bandwidths are used, as is often desirable to achieve additional diversity benefit. Furthermore, in deriving the corresponding optimum equalizers, we exploit the fact that in this case the fading process becomes increasingly slowly varying as the bandwidth is expanded.

Accordingly, we begin by assuming that the coherence time in the channel is large, so that the fading coefficients are effectively constant over a several time-samples. Then the time-variant channel frequency response $A(\omega; n]$ will vary slowly with n, and admissible equalizers will also have a slowly varying time-variant frequency response $B(\omega; n]$. Furthermore, we have

$$C(\omega; n] \approx A(\omega; n]\, B(\omega; n]. \tag{33}$$

Now (19) and (23) imply

$$\mu_c = E[C(\omega; n]] \tag{34a}$$

$$\sigma_c^2 = \text{var}\,[C(\omega; n]] \tag{34b}$$

and

$$\sigma_b^2 + |\mu_b|^2 = E\big[|B(\omega; n]|^2\big]. \tag{34c}$$

Hence, using (34) with (33) in (27), we get that the channel SNR is effectively given by

$$\gamma(b) \approx \frac{|E[AB]|^2}{\text{var}\,[AB] + \xi_0 E[|B|^2]} \tag{35}$$

where, again, ξ_0 is as given by (28), and where we have omitted specification of both the time sample n and frequency value ω due to stationarity. Clearly, (35) is identical in form to (29), and, consequently, the equalizer providing the best SNR for the composite channel follows analogously as

$$B(\omega; n] \propto \frac{A^*(\omega; n]}{|A(\omega; n]|^2 + \xi_0} \tag{36}$$

where, again, the (complex) constant of proportionality is arbitrary. As in the nonselective fading case, we remark that this equalizer not only maximizes the channel SNR but also, when suitably normalized, makes $\hat{x}[n]$ a minimum mean-square-error linear estimate of $x[n]$.

The receiver structure in this frequency-selective scenario warrants some additional discussion. With $b[n; k]$ varying slowly with n, let us denote by $b[k]$ the nominal value of $b[n; k]$ over some sufficiently long generic time interval. To implement the unit-sample response $b[k]$, it is useful, at least conceptually, to view the equalization process in two stages. The first stage implements the numerator of (36), and corresponds to the appropriate matched-filter equalizer, and, hence, is a conventional RAKE receiver [1]. The unit-sample response of this stage is, therefore, $a^*[-k]$. The second stage, which implements the denominator of (36), then performs additional compensation, taking into account the SNR in the channel. The unit-sample response corresponding to this second stage, which we denote by $e[k]$, is symmetric and, in general, infinite in extent (hence, two-sided), precluding any recursive implementation. However, typically, the tails of the unit-sample response fall off quickly. In particular, when $a[k]$ is nonzero for only finitely many values of k as is frequently assumed in practice, $e[k]$ decays exponentially quickly with k. Hence, using truncation $e[k]$ may be effectively approximated as a symmetric FIR filter. As an example, Fig. 2 depicts the normalized RMS value of the coefficient $e[k]$, viz.

$$\sqrt{E[|e[k]|^2]/E[|e[0]|^2]}$$

as a function of k, where

$$E\big[|a[k]|^2\big] = \begin{cases} 1/2, & k = 0, 1 \\ 0, & \text{otherwise} \end{cases} \tag{37}$$

and where $\xi_0 = \sigma_a^2$.

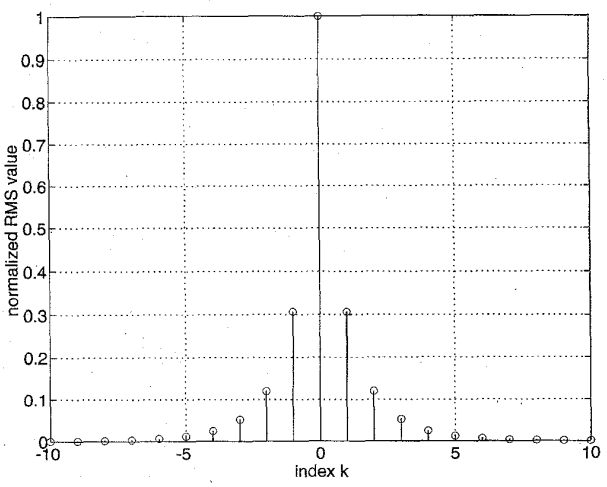

Fig. 2. A typical RMS unit-sample response of the second stage of equalizer. In this example, the variances of the fading coefficients $a[k]$ were chosen according to (37), and the SNR was chosen so that $\xi_0 = \sigma_a^2$.

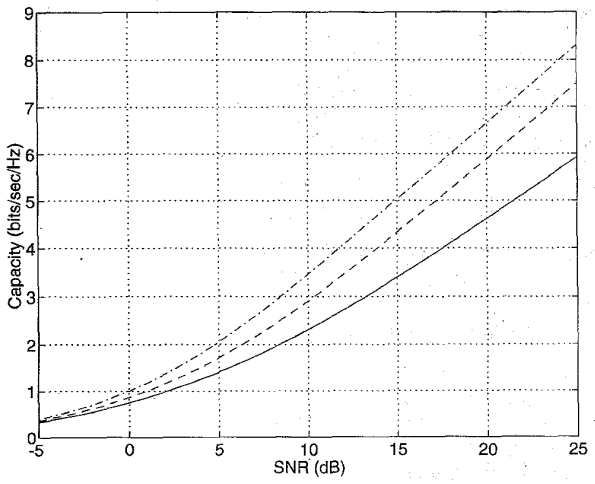

Fig. 3. Capacity estimates, Rayleigh fading channel. The solid curve is the capacity estimate C determined using precoding. For comparison, the dash-dotted curve is the capacity C_∞ when infinite spatial diversity is available, while the dashed curve is the capacity estimate C_0 due to Lee [13].

V. Performance

In this section, we explore the potential performance achievable through the use of spread-response precoding with optimized receivers. We begin by observing that with the optimum equalizer, i.e., (32) in the case of frequency-nonselective fading or (36) in the case of frequency-selective fading, we readily obtain that the corresponding SNR in the composite channel is given by

$$\gamma_0 = \frac{1}{E\left[\frac{1}{\alpha_0+1}\right]} - 1 \tag{38}$$

where[4]

$$\alpha_0(\omega; n] = \frac{|A(\omega; n]|^2 \mathcal{E}_s}{\mathcal{N}_0 \mathcal{W}_0} \tag{39}$$

denotes the SNR in the original fading channel at a particular time instant n and frequency ω. A useful notion of the capacity of the composite channel is given by the equivalent Gaussian capacity,[5] i.e., using (38)

$$C/\mathcal{W}_0 = \log(1+\gamma_0) = -\log\left(E\left[\frac{1}{\alpha_0+1}\right]\right). \tag{40}$$

Exploiting the easily verified identity

$$E[\log(\alpha_0+1)] = \frac{1}{\zeta_0} E\left[\frac{1}{\alpha_0+1}\right] = e^{\zeta_0} E_1(\zeta_0) \tag{41}$$

where

$$1/\zeta_0 \triangleq E[\alpha_0] = \frac{\sigma_a^2 \mathcal{E}_s}{\mathcal{N}_0 \mathcal{W}_0} \tag{42}$$

denotes the average SNR in the original fading channel (cf. (46)), and $E_1(\cdot)$ denotes the exponential integral [12]

$$E_1(\nu) = \int_\nu^\infty \frac{e^{-t}}{t}\, dt \tag{43}$$

we get that (40) can be expressed more conveniently as

$$C/\mathcal{W}_0 = -\log\left(\zeta_0 e^{\zeta_0} E_1(\zeta_0)\right). \tag{44}$$

The capacity estimate (44) can be compared to some related capacity calculations. In particular, by the Schwarz inequality we get

$$E\left[\frac{1}{\alpha_0+1}\right] \geq \frac{1}{E[\alpha_0+1]} = \frac{1}{1+1/\zeta_0}$$

so that, as expected, (44) is upper-bounded by the capacity of the Gaussian channel or, equivalently, the fading channel with infinite spatial diversity, i.e.

$$C_\infty/\mathcal{W}_0 = \log(1+E[\alpha_0]) = \log(1+1/\zeta_0). \tag{45}$$

More generally, there have been a variety of attempts to estimate the capacity of fading channels in the literature [6]. As an example, between C and C_∞ lies the estimate of fading channel capacity without spatial diversity derived by Lee [13], i.e.

$$C_0/\mathcal{W}_0 = E[\log(1+\alpha_0)] = e^{\zeta_0} E_1(\zeta_0) \tag{46}$$

where the second equality follows from (41). In Fig. 3, these capacity estimates (in bits per second per hertz) are plotted as a function of the average available SNR. The capacities C, C_0, and C_∞ are represented by the solid, dashed, and dash-dotted curves, respectively.

At high SNR (i.e., small ζ_0), we can use the series expansion [12]

$$E_1(\nu) = -\Gamma_0 - \log\nu - \sum_{k=1}^{\infty} \frac{(-1)^k \nu^k}{k\, k!} \tag{47}$$

[4]Of course, in the case of nonselective fading $A(\omega; n] = a[n; 0] = a[n]$ using the notation of Section IV-A.

[5]More precisely, this can be interpreted as a constrained capacity—specifically the bit rate that can be achieved when the remaining higher order statistical dependencies in the composite channel model are not exploited.

where $\Gamma_0 = 0.57721\cdots$ is Euler's constant, to show that (44) is given asymptotically by

$$\mathcal{C}/\mathcal{W}_0 \sim \log\left(\frac{1/\zeta_0}{\log(1/\zeta_0)}\right). \tag{48}$$

By contrast, in the same regime (45) behaves like

$$\mathcal{C}_\infty/\mathcal{W}_0 \sim \log(1/\zeta_0) \tag{49}$$

while (46), as can be shown via (47), satisfies

$$\mathcal{C}_0/\mathcal{W}_0 \sim \Gamma_0 + \log(1/\zeta_0). \tag{50}$$

Hence, comparing (50) with (49) and (48) we can verify that at high SNR the difference between $\mathcal{C}_\infty$ and $\mathcal{C}_0$ is $10\Gamma_0 \log e \approx 2.506$ dB while the difference between $\mathcal{C}_0$ and $\mathcal{C}$ diverges to infinity.

We stress that these capacity estimates correspond to the case in which the transmitter has no knowledge of the state of the fading channel or its statistics at any point in time, i.e., there is no side-channel for feedback from the receiver to the transmitter. We note, however, because of memory in the fading channel, the availability of a feedback path would naturally lead to higher capacity [14].

We also remark that to approach the capacity $\mathcal{C}$ of the composite channel requires, of course, that coding be applied to the data stream prior to precoding. However, because the composite channel is effectively an additive white Gaussian noise channel, any of the traditional forms of coding for this channel would be appropriate. In particular, we note that conventional implementations of trellis-coded modulation appear to be well-suited to this scenario.

Nevertheless, even without coding significant improvements in bit error rate performance can be achieved from the inherent diversity benefit of using spread-response precoding. We emphasize that this is in marked contrast to the use of interleaving, which offers no improvement in bit error rate performance without coding. For the purposes of illustration, let us consider the case in which $x[n]$ is an uncoded QPSK (quadrature phase-shift keying) stream. When precoding is used, the bit error probability as a function of the SNR per bit, i.e.

$$\frac{\mathcal{E}_b\sigma_a^2}{\mathcal{N}_0\mathcal{W}_0} = \frac{\mathcal{E}_s\sigma_a^2}{2\mathcal{N}_0\mathcal{W}_0}$$

is given by

$$\mathcal{P} = \mathcal{Q}(\sqrt{\gamma_0}) \tag{51}$$

where

$$\mathcal{Q}(\nu) = \frac{1}{\sqrt{2\pi}}\int_\nu^\infty e^{-t^2/2}\,dt$$

and where γ_0, via (38) with (39), is given by

$$\gamma_0 = \frac{1}{\zeta_0\, e^{\zeta_0}\, E_1(\zeta_0)} - 1$$

with ζ_0 given by (42).

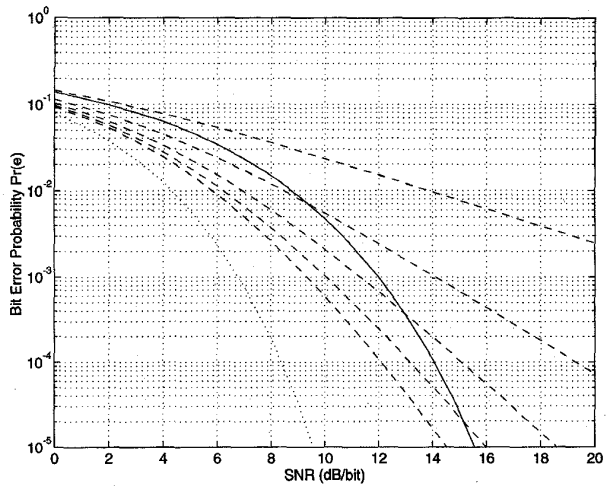

Fig. 4. Bit error probabilities using uncoded QPSK on the Rayleigh fading channel. The solid curve represents the performance achievable with precoding. For comparison, also depicted is the attainable performance without precoding but, instead, with spatial diversity and maximal ratio combining. The dotted curve corresponds to the performance with infinite spatial diversity, while the successively lower dashed curves correspond to the performance with $L = 1, 2, \cdots, 5$ branches of spatial diversity, respectively.

For comparison, without precoding the QPSK bit error probability using L-fold spatial diversity and maximal ratio combining is given by [1]

$$\mathcal{P}_0[L] = \frac{1}{2}\left[1 - \frac{1}{\sqrt{2\zeta_0 L + 1}}\sum_{k=0}^{L-1}\binom{2k}{k}\left(\frac{\zeta_0 L}{2(2\zeta_0 L + 1)}\right)^k\right]. \tag{52}$$

Furthermore, (52) specializes to

$$\mathcal{P}_0[1] = \frac{1}{2}\left(1 - \frac{1}{\sqrt{2\zeta_0 + 1}}\right) \tag{53}$$

when there is no spatial diversity, and to

$$\mathcal{P}_0[\infty] = \mathcal{Q}\left(\sqrt{E[\alpha_0]}\right) = \mathcal{Q}\left(1/\sqrt{\zeta_0}\right) \tag{54}$$

when there is infinite spatial diversity. We stress that the bit error rates (52), and their special cases (53) and (54), are the best that can be achieved in uncoded QPSK systems—in particular for the optimum choice of equalizer. As such it is useful to compare the performance of these systems to that of precoded systems with their optimum equalizers.

In Fig. 4, we plot bit error probability as a function of SNR per bit (i.e., $1/(2\zeta_0)$) with and without precoding. The solid curve in Fig. 4 corresponds to the use of precoding (with infinite dispersion) but no spatial diversity. The dashed curves correspond to the use of no precoding but L-fold diversity for $L = 1, 2, \cdots, 5$. Finally, the dotted curve corresponds to the use of no precoding but infinite spatial diversity, $L \to \infty$.

Comparing $\mathcal{P}$ with $\mathcal{P}_0[1]$ we see that precoding markedly improves bit error rate performance in the channel. We can further show, by applying (47) and the asymptotic expansion [12]

$$\mathcal{Q}(\nu) \sim \frac{1}{\sqrt{2\pi}\nu}e^{-\nu^2/2}\sum_{k=0}^{\infty}\frac{(-1)^m\,(2m)!}{2^m\,m!}\,\nu^{-2m} \tag{55}$$

to (51), that at high SNR (i.e., small ζ_0) the bit error rate with precoding is given by

$$\mathcal{P} \sim \sqrt{\frac{\log(1/\zeta_0)}{1/\zeta_0}} \exp\left(-\frac{1/(2\zeta_0)}{\log(1/\zeta_0)}\right). \tag{56}$$

By contrast, in the high SNR regime, $\mathcal{P}_0[L]$ is well-approximated as [1]

$$\mathcal{P}_0[L] \sim \zeta_0^L$$

while (54), via (55), takes the form

$$\mathcal{P}_0[\infty] \sim \sqrt{\zeta_0} e^{-1/(2\zeta_0)}.$$

Thus we note that the while $\mathcal{P}$ falls off at a slower rate than $\mathcal{P}_0[\infty]$, it falls off faster than $\mathcal{P}_0[L]$ for any fixed L. This implies that, asymptotically, precoding provides higher "effective diversity" than can be achieved using spatial diversity with any $L < \infty$, but less than can be achieved with infinite spatial diversity. That the dotted curve (infinite spatial diversity) is lower than the solid curve (infinite temporal diversity) is due to unavoidable intersymbol interference effects in the latter.

The reader is cautioned from inferring more than is appropriate from Fig. 4, since direct comparisons between spatial diversity strategies and temporal diversity strategies naturally provide only limited insight. For example, it should be emphasized that in spatial diversity, schemes are effective even when the coherence time of the channel is infinite (e.g., when a mobile is stationary), whereas temporal diversity strategies provide no benefit in such scenarios. From this perspective, we note that the ergodicity requirements in Theorem 1 would not be realistic in mobile communications scenarios where the mobiles are stationary. More generally, these ergodicity assumptions may not be realistic for some classes of nonstationary channels that arise in practice.

Finally, we remark that experiments exploring the sensitivity of system performance to the parameters of the equalizer, while beyond the scope of this paper, are clearly warranted in the future. In the meantime, preliminary simulations reported in [4] involving minimum-mean-square-error-type equalizers lend at least some insight into what kind of behavior may be expected. Specifically, the results suggest that performance ought to depend only weakly on the estimate of $\mathcal{E}_s/(\mathcal{N}_0\omega_0)$ used in the equalizer, and that the performance can be expected to degrade fairly gracefully with errors in estimates of the magnitude and phase of the fading coefficients.

VI. Precoder Design Issues

All of the preceding results are asymptotic in the sense that they correspond to the use of ideal precoders. However, ideal precoders are lossless and perfectly dispersive, implying infinite length (and, hence, delay). In this section, we explore some of the considerations in the design of practical finite-delay precoders, and in addition present some *ad hoc* strategies for optimizing the loss characteristics of such precoders.

First, we discuss the impact of channel coherence time on precoder design. We begin by observing that although Theorem 1 is an asymptotic result, with suitably chosen finite-length precoders, the white marginally Gaussian channel model can be an extremely useful approximation to the actual composite channel. Furthermore, the delay requirements in this case are comparable to those of conventional interleaving. Specifically, the filter length N required to effectively converge to the equivalent model is given by

$$N \approx N'(\tau_a + 1) \tag{57}$$

where N' is the length required in the case of memoryless fading, and where τ_a is the coherence time of the fading channel (in samples). Specifically

$$\tau_a = \frac{1}{\sigma_a^2}\sum_{m=1}^{\infty} \Re e\{\Psi_a(0;m]\} = \left(\frac{1}{\sigma_a^2}\sum_{m=-\infty}^{+\infty} \Psi_a(0;m]\right) - 1 \tag{58}$$

where, defined according to (20), $\Psi_a(\omega;m]$ is the original channel's spaced-frequency spaced-time correlation function. Later we discuss appropriate values for N' in practice.

It is important to note that while large coherence times (or, equivalently, small Doppler spreads) correspond to larger inherent delays in the system, they need not incur additional computational complexity either at the transmitter or receiver. In fact, from a single prototype precoder $h[n]$ one can derive an entire family of precoders with the same loss, dispersion, energy, and computational characteristics but suitable for scenarios corresponding to different coherence–time/Doppler-spread parameters. Specifically, if $h[n]$ is a precoder designed for memoryless fading ($\tau_a = 0$), then the corresponding precoder $h_{\tau_a}[n]$ for the case in which the fading has coherence time τ_a is obtained by simply upsampling $h[n]$, i.e.

$$h_{\tau_a}[n] = \begin{cases} h[n/M], & n = \cdots, -M, 0, M, 2M, \cdots \\ 0, & \text{otherwise} \end{cases} \tag{59}$$

where[6]

$$M = \lceil \tau_a + 1 \rceil$$

is the upsampling factor. Equivalently, this upsampling relationship can be described in the frequency domain as

$$H_{\tau_a}(\omega) = H(M\omega). \tag{60}$$

Using both (59) and (60) one can verify that the energy, loss, dispersion, and computational characteristics are unaffected by such upsampling.

Let us next turn to a discussion of the optimization of finite-length precoders, and begin by observing that in general, overall system performance depends in a rather complicated manner on the loss and dispersion characteristics of the precoding filter. Furthermore, even if a weighted combination of the losslessness and dispersion factors were to correspond to some reasonable measure of ultimate system performance, optimizing such a criterion is an intrinsically difficult numerical problem.

Nevertheless, there are a number of approaches that work well in practice for obtaining precoding filters corresponding to a reasonable compromise between losslessness and dispersion

[6]The ceiling function $\lceil x \rceil$ denotes the smallest integer greater than or equal to x.

factors, and providing good overall system performance. In fact, design techniques are suggested from a variety of sources, largely because such filters find application in a number of distinct communication problems ranging from the mitigation of impulse noise in communication systems [15] to robust quantization of non-Gaussian sources [16]. Those we discuss here are closely related to the techniques which have proven useful in these problems.

As discussed earlier, binary precoders have attractive computational properties and optimal dispersion factors but poor losslessness factors. The binary sequences having optimal losslessness factors for a given length constraint N are tabulated[7] in [17] for $N \leq 71$. For length $N = 13$, the corresponding sequence is, for example, the well-known Barker sequence for which $\mathcal{L}_h \approx 14.08$. Likewise, for length $N = 27$, the optimum sequence has $\mathcal{L}_h \approx 9.85$. Another class of binary sequences with better-than-average losslessness characteristics are the maximal length shift-register sequences (or m-sequences) [18], for which $\mathcal{L}_h \sim 3$ for large N as shown in [19].

In practice, the losslessness characteristics of these sequences can be markedly improved while largely preserving their dispersion properties by relaxing their binary amplitude constraints in a controlled manner. One way to accomplish this is to apply the following simple heuristic algorithm. Beginning with an initial binary sequence $h_0[n]$, we proceed to maximize $\mathcal{L}_h$ in the form (10) via an iterative ascent algorithm (such as the Simplex method) subject to the unit-energy constraint (9). Naturally, a global optimization would result in the trivial solution $\delta[n]$. However, the objective function typically has many local maxima, and in practice, the algorithm generally converges to such a fixed point, and results in a filter with substantially improved $\mathcal{L}_h$ at a relatively modest cost in $\mathcal{D}_h$.

Other filters with reasonable dispersion factors are also suitable as an initialization for this type of algorithm. For instance, in [16] a chirp sequence of the form

$$h_0[n] = \beta \sin\left[\frac{\pi n(n-1)}{2N}\right], \quad \text{for } n = 0, 1, \cdots, N-1$$

is used with good results. This initialization is especially useful in the design of very long precoders, in which case the corresponding optimal binary sequences are unknown. However, depending on the specific value of N and on the specific iterative descent algorithm, certain initializations lead to better precoders than others in terms of overall system performance. Consequently, trial and error is invariably involved.

Again we emphasize that the performance results developed in Section V are asymptotic results, i.e., they apply to infinite length (and hence delay) precoders. From this perspective, the solid curve in Fig. 4 is obviously a lower bound on the bit error rate performance achievable in practice using finite length precoders. In Fig. 5, we plot bit error probability for uncoded QPSK as a function of SNR per bit using realizable precoders. The uppermost curve indicates the performance without precoding ($N' = 1$) while the lowermost curve indicates the performance bound corresponding to infinite-length precoders ($N' \to \infty$). The successively lower curves between these two extremes indicate the performance with practical precoders corresponding to $N' = 13$, $N' = 27$, and $N' = 200$, respectively. The coefficients of these precoders, together with a description of how they were designed, are provided for reference in Appendix II. Since system delay is proportional to N' as we have discussed, Fig. 5 indicates how achievable performance varies as a function of delay, normalized by the coherence time of the channel. From Fig. 5 we can also conclude that the asymptotic solid curve in Fig. 4 is a close approximation to what is attained in practice when the precoding filter has length N given by (57) for $N' \approx 100$. However, such extreme delays are likely to be intolerable in many applications.

[7] Actually, to simplify the search for such sequences, typically only skew-symmetric binary sequences are considered. This restriction is not severe, however, since this class generally includes many of the best sequences even when the restriction is removed.

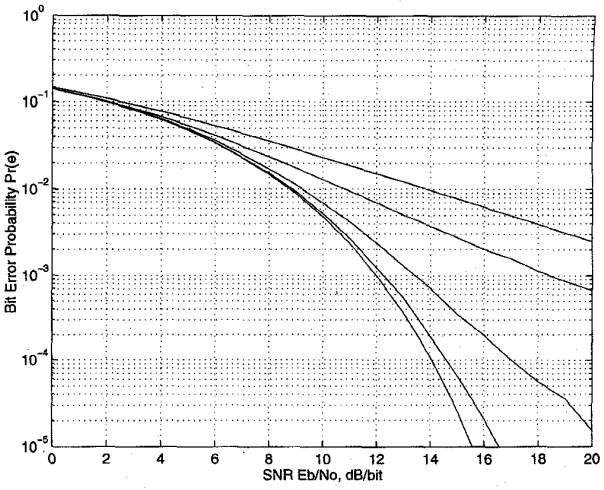

Fig. 5. Bit error probabilities using uncoded QPSK on the Rayleigh fading channel with realizable precoders. The top curve corresponds to the performance without precoding ($N' = 1$), while the bottom curve indicates the performance bound corresponding to an infinite-length (delay) precoder ($N' \to \infty$). The successively lower curves between these two extremes represent the performance obtained using FIR precoders with length (delay) parameters $N' = 13$, $N' = 27$, and $N' = 200$, respectively.

VII. Concluding Remarks

Spread-response precoding as developed in this paper constitutes a potentially attractive alternative to interleaving in a wide range of communication systems designed for use with multipath fading channels. Even when no additional coding is used, precoding can significantly improve system performance over other uncoded systems. Similarly, the use of precoding in conjunction with coding has the potential to substantially reduce computational complexity at both the transmitter and the receiver for a given level of performance. This is because the effects of fading are entirely controlled by the precoding, which requires only low-complexity signal processing. Thus, only additive noise remains for coding to control, which can in turn be achieved with comparatively shorter codes. As an additional potential feature, the noise-like characteristics of the transmitted stream resulting from the use of precoding appears to be well-suited for applications involving secure communication.

Nevertheless, several technical issues remain to be explored. For example, a thorough investigation of the complexity benefits that can be realized through the use of precoding with coding is clearly warranted. The development of techniques for adequately synchronizing the receiver in such systems as well as for managing the inherent peak-to-average power requirements is also an important avenue for future research. Furthermore, in order for precoding to be effective, reliable estimates of the fading channel parameters and statistics must be available at the receiver. It would appear that this can be accomplished in practice through the use of training sequences or decision feedback techniques. However, such issues remain to be explored in detail. Finally, as remarked earlier, regardless of the technique used, any such parameter estimates are imperfect and, as a result, a thorough sensitivity analysis would ultimately be important in further verifying the viability of spread-response precoding.

APPENDIX I
PROOF OF THEOREM 1

As an intermediate step, we obtain results concerning the following related system. Let $\mathcal{S}\{\cdot\}$ denote a linear system which is the cascade of an LTI system whose (real) unit-sample response is $g_1[n]$, followed by a linear system whose (complex) response at time n to an unit-sample at time $n-k$ is $f[n;k]$, followed by another LTI system whose (real) unit sample response is $g_2[n]$. Hence

$$\begin{aligned} q[n] &= \mathcal{S}\{p[n]\} \\ &= \sum_i g_2[i] \sum_k f[n-i;k] \sum_l g_1[l]\, p[n-i-k-l]. \end{aligned} \tag{61}$$

Furthermore, let $u[n;k]$ denote the kernel of the overall linear system, i.e., its response at time n to a unit-sample at time $n-k$.

We begin with a useful lemma regarding such systems.

Lemma 1: Let $g_1[n]$ and $g_2[n]$ be lossless, and let $f[n;k]$ be the kernel of an admissibly ergodic system. Then as

$$\mathcal{D}_2 = \left(\sum_i g_2^4[i] \right)^{-1} \to \infty \tag{62}$$

the kernel $u[n;k]$ defined above obeys

$$u[n;k] \xrightarrow{\text{m.s.}} \mu\,(g_1[k] * g_2[k]) \triangleq u[k] \tag{63}$$

and

$$\sum_k \tilde{u}[n;n-k]\, \tilde{u}^*[m;m-k] \xrightarrow{\text{m.s.}} \sigma^2 \delta[n-m] \tag{64}$$

where

$$\tilde{u}[n;k] = u[n;k] - u[k].$$

TABLE I
COEFFICIENTS OF PRECODER WITH $N' = 13$

n	$h[n]$	n	$h[n]$
0	-5.8411858005023801e-03	7	-3.1185041135844094e-01
1	2.4550906513458115e-03	8	1.7981312791890364e-01
2	4.0809152050496414e-02	9	-8.2661635586315216e-02
3	-1.4930692875175594e-01	10	3.2767268474091955e-02
4	-6.7555021202975918e-01	11	-1.0462535657742033e-02
5	-4.4807541797136691e-01	12	2.3742704387674806e-03
6	4.2575301996495318e-01		

Proof: From (61) we get

$$u[n;k] = \sum_i g_2[i] \sum_l f[n-i;l]\, g_1[k-i-l]. \tag{65}$$

Then

$$E[u[n;k]] = \mu \sum_i g_2[i]\, g_1[k-i] = \mu_c \cdot g_1[k] * g_2[k]$$

and

$$\tilde{u}[n;k] = \sum_i g_2[i] \sum_l \tilde{f}[n-i;l]\, g_1[k-i-l]$$

where, consistent with (14),

$$\tilde{f}[n;k] = f[n;k] - \mu\, \delta[k].$$

Hence

$$\begin{aligned} &E\left[|\tilde{u}[n;k]|^2\right] \\ &\quad = \sum_{i,i'} \sum_l g_2[i]\, g_2[i']\, R[i'-i;l]\, g_1[k-l-i]\, g_1[k-l-i'] \end{aligned} \tag{66}$$

where $R[m;k]$ is as defined in (17b). Applying, in order, the triangle inequality and the Cauchy inequality, we are able to bound (66) by

$$E\left[|\tilde{u}[n,k]|^2\right] \le \varphi(g_1)\, \varphi(g_2) \tag{67}$$

where

$$\varphi^2(g) = \sum_{i,i',l} |R[i'-i;l]| g^2[i]\, g^2[i'] \le S_R$$

provided

$$\sum_n g^2[n] \le 1.$$

Applying the Cauchy inequality again to $\varphi^2(g_2)$, however, gives, after some simplification and using (62)

$$\varphi^2(g_2) \le S_R/\mathcal{D}_2. \tag{68}$$

Hence, (68) and, in turn, (66) tend to zero as $\mathcal{D}_2 \to \infty$, which verifies (63).

To show (64), we begin by noting that since $g_1[n]$ is lossless, we get, using (15),

$$\begin{aligned} \rho[n,m] &\triangleq \sum_k \tilde{u}[n;n-k]\, \tilde{u}^*[m;m-k] \\ &= \sum_{i,l} g_2[n-i]\, g_2[m-i+l]\, d[i;l]. \end{aligned}$$

TABLE II
COEFFICIENTS OF PRECODER WITH $N' = 27$

n	$h[n]$	n	$h[n]$	n	$h[n]$
0	-9.9015416362696340e-02	9	-2.1507649306322030e-01	18	2.2770635469845774e-01
1	-1.4962526200154719e-01	10	1.3465094288183066e-01	19	-1.6416819374047256e-01
2	-1.2494634826461959e-02	11	-2.0888931073231989e-01	20	-1.0105982280370986e-01
3	1.5310948500665450e-01	12	-2.3723201347398892e-01	21	2.4568799799401064e-01
4	2.8095844765330646e-01	13	-2.8141046006102444e-01	22	-2.9580333293734362e-01
5	1.9088320211272225e-01	14	2.4456267753644959e-01	23	1.6617449019023858e-01
6	8.5047173390195421e-02	15	-1.7757930264336236e-01	24	5.5625529622671227e-02
7	-2.5661278692721445e-01	16	-1.2222751930073791e-01	25	-1.6595106517284344e-01
8	-2.7249797704898165e-01	17	-1.4688495027957671e-01	26	1.1775033638223745e-01

Then, since by (17b), (22), and (23)

$$E[d[n;k]] = \sigma^2\,\delta[k]$$

we get, since $g_2[n]$ is lossless,

$$E[\rho[n,m]] = \sigma^2\,\delta[n-m].$$

Next, we write, using (16)

$$\begin{aligned}\tilde{\rho}[n,m] &\triangleq \rho[n,m] - \sigma^2\delta[n-m] \\ &= \sum_{i,l} g_2[n-i]\,g_2[m-i+l]\,\tilde{d}[i;l]\end{aligned}$$

and, using (17c)

$$\begin{aligned}E\left[|\tilde{\rho}[n,m]|^2\right] = \sum_{i,i',l,l'} & g_2[n-i]\,g_2[m-i+l] \\ & \cdot g_2[n-i']\,g_2[m-i'+l']\,T[i-i';l,l']. \quad (69)\end{aligned}$$

However, applying the triangle and Cauchy inequalities, in order, and noting

$$T[m;k,l] = T^*[-m;l,k]$$

we can bound (69) by

$$E\left[|\tilde{\rho}[n,m]|^2\right] \le \sum_{i,i',l,l'} g_2^2[n-i]\,g_2^2[m-i+l]\,|T[i-i';l,l']|. \quad (70)$$

Applying the triangle and Cauchy inequalities, in order, again, to the right side of (70), and changing variables, we get

$$E\left[|\tilde{\rho}[n,m]|^2\right] \le \sum_{i,i',l,l'} g_2^4[i]|T[i';l,l']| = S_T/\mathcal{D}_2 \quad (71)$$

which approaches zero as $\mathcal{D}_2 \to \infty$. □

Using Lemma 1, we obtain the following theorem:

Theorem 2: Let $g_1[n]$ and $g_2[n]$ be lossless, and let $f[n;k]$ be an admissibly ergodic system kernel. Further, and suppose $p[n]$ is a wide-sense-stationary, white random process with mean zero and variance σ_p^2, and that $p[n]$ and the channel kernel $f[n;k]$ are statistically independent. Then, as $\mathcal{D}_2 \to \infty$, $q[n]$ as defined by (61) satisfies, with $u[n]$ as defined in (63)

$$q[n] \xrightarrow{\text{m.s.}} u[n] * p[n] + z[n] \quad (72)$$

where $z[n]$ is a marginally Gaussian wide-sense-stationary, white random process with mean zero and variance $\sigma^2 c_p^2$, and where $z[n]$ is uncorrelated with $p[n]$.

Proof: By superposition

$$q[n] = \sum_k u[n;k]\,p[n-k]$$

hence

$$z[n] = q[n] - u[n] * p[n] = \sum_k \tilde{u}[n;k]\,p[n-k]. \quad (73)$$

From (73) we get immediately, since $p[n]$ is zero-mean

$$E_p[z[n]] = 0$$

where we use $E_p[\cdot]$ to denote expectation with respect to $p[n]$ given a fixed but arbitrary realization of the kernel $f[n;k]$.

In addition, from (73) we get

$$\begin{aligned}E_p[z[n]\,p^*[m]] &= \sum_k \tilde{u}[n;k]\,E_p[p[n-k]\,p^*[m]] \\ &= \sigma_p^2\tilde{u}[n;n-m]. \quad (74)\end{aligned}$$

Hence, since (63) in Lemma 1 implies

$$\tilde{u}[n;k] \xrightarrow{\text{m.s.}} 0 \;\text{ as }\; \mathcal{D}_2 \to \infty$$

we get from (74)

$$E_p[z[n]\,p^*[m]] \xrightarrow{\text{m.s.}} 0 \;\text{ as }\; \mathcal{D}_2 \to \infty\,.$$

Finally, using (73) we also obtain

$$\begin{aligned}E_p[z[n]\,z^*[m]] &= \sum_{k,l} \tilde{u}[n;k]\,\tilde{u}^*[m;l]E_p[p[n-k]\,p^*[m-l]] \\ &= \sigma_p^2 \sum_k \tilde{u}[n;n-k]\,\tilde{u}^*[m;m-k]. \quad (75)\end{aligned}$$

Applying (64) in Lemma 1 to (75), we see immediately

$$E_p[z[n]\,z^*[m]] \xrightarrow{\text{m.s.}} \sigma^2\sigma_p^2\delta[n-m] \;\text{ as }\; \mathcal{D}_2 \to \infty\,.$$

Finally, to show that $z[n]$ is marginally Gaussian requires a Central Limit Theorem argument. □

The following corollaries lead directly to a proof of our main theorem.

Corollary 1: Suppose $g_1[n] = g_2[-n]$ in Theorem 2. Then as $\mathcal{D}_2 \to \infty$

$$q[n] \xrightarrow{\text{m.s.}} \mu\,p[n] + z[n]. \quad (76)$$

TABLE III
COEFFICIENTS OF PRECODER WITH $N' = 200$

n	$h[n]$	n	$h[n]$	n	$h[n]$
0	6.7481759487174279e-03	67	-1.9812865943925784e-02	134	6.7742129938659024e-02
1	6.2399846643046283e-03	68	-6.5158588465724657e-02	135	-3.8687441526780691e-02
2	2.3121320489424739e-03	69	-6.0671964289127335e-02	136	-2.5257690444906160e-02
3	-2.1211506895814540e-03	70	-5.8502372962630301e-03	137	5.1191350115345584e-02
4	3.5102254094720173e-04	71	7.4961066626407058e-02	138	-4.2680062356762853e-02
5	4.9937802628538912e-03	72	7.2081840324012825e-02	139	-4.2119123303270859e-03
6	1.4984053323151954e-02	73	-3.8878837530640788e-02	140	9.1740729473087229e-02
7	2.5203915461724336e-02	74	-9.3785655315623093e-02	141	-1.2639520276889260e-01
8	3.9798349600777438e-02	75	-4.8648827925370244e-02	142	3.8437811184807144e-02
9	5.5551183441289842e-02	76	5.6955491301629524e-02	143	7.8142875235300086e-02
10	6.7288182918999545e-02	77	1.2316803297557807e-01	144	-1.1452645727161301e-01
11	9.0392651115411560e-02	78	1.5387319674599003e-02	145	7.6485962980356953e-02
12	1.2050201278976566e-01	79	-1.2293448245238595e-01	146	-4.1513288095059190e-03
13	1.3319069287581600e-01	80	-7.9990444425209556e-02	147	-6.5221324247226389e-02
14	1.2941965652091353e-01	81	7.4049574737542784e-02	148	8.0068586977575254e-02
15	1.2869085815897530e-01	82	1.0057295318039847e-01	149	-2.7427212758030589e-02
16	1.2883748628498681e-01	83	-5.7613802110531836e-03	150	-3.9649334610519296e-02
17	1.1207361561371065e-01	84	-8.7898534630834940e-02	151	7.4311438031468946e-02
18	7.5770772973918196e-02	85	-4.2790572645302158e-02	152	-6.8324453161421245e-02
19	3.2171594752145573e-02	86	6.8875940510299216e-02	153	2.1265783767044862e-02
20	8.7158815307746551e-03	87	5.5918915180891579e-02	154	5.5255938046250050e-02
21	7.4800978349197052e-03	88	-3.7418688847588095e-02	155	-1.0812107916172052e-01
22	-4.8356918721120124e-03	89	-7.7219864077822525e-02	156	1.0433507079345014e-01
23	-3.8648910229053639e-02	90	3.8475560784670404e-03	157	-6.3041542086211766e-02
24	-7.8362676756697849e-02	91	1.0051646628831766e-01	158	-8.4762023687665403e-04
25	-9.1879216789721246e-02	92	2.6585413581657308e-02	159	8.3391803227558570e-02
26	-7.6277974846228738e-02	93	-9.3086565360855439e-02	160	-1.3663301918921161e-01
27	-4.6401505563091174e-02	94	-4.8247900353889150e-02	161	1.1640358139880574e-01
28	-1.9275653906712049e-02	95	8.4497553917583901e-02	162	-5.3459874620862345e-02
29	9.3872778388958307e-03	96	4.2292822933925084e-02	163	1.5692615498749335e-03
30	4.9958428365860480e-02	97	-7.1804994558062135e-02	164	3.9671816576985652e-02
31	8.2664124686710333e-02	98	-4.2172204658277881e-02	165	-8.0702853067170566e-02
32	9.1647925938961164e-02	99	6.0183037953395940e-02	166	1.0554972708952620e-01
33	6.7983526073862433e-02	100	6.4238065492258398e-02	167	-9.0224086359934313e-02
34	3.4040998868462270e-02	101	-7.7180841048434062e-02	168	3.9366214767518434e-02
35	-4.9145491606543638e-03	102	-4.7816597407733689e-02	169	1.0166816185420646e-02
36	-5.8885351510306584e-02	103	7.3106003333906405e-02	170	-3.0671765812497406e-02
37	-1.0103817084231298e-01	104	2.6381717497109474e-02	171	3.8010890554600614e-02
38	-9.8138351826530884e-02	105	-6.1794082890507113e-02	172	-5.6882677375084026e-02
39	-5.4534429214527766e-02	106	-3.4127365748038485e-02	173	6.8870641150388101e-02
40	-1.4933548278368292e-02	107	9.8844539751448440e-02	174	-5.3600301902024840e-02
41	2.5962761620815004e-02	108	2.0277700593667149e-02	175	2.5191115869247566e-02
42	8.3123979384541913e-02	109	-1.2805057651021626e-01	176	-3.0378475939394102e-17
43	1.1808609119356409e-01	110	6.3400166096573064e-04	177	-2.3783861299020385e-02
44	9.1789254030566064e-02	111	1.2564583308008287e-01	178	3.3660425705331322e-02
45	1.6960452014801397e-02	112	-1.7091309884048406e-02	179	-3.0434462069177784e-02
46	-5.6810317206874683e-02	113	-1.1038360258378160e-01	180	3.1545001332020539e-02
47	-1.1070595506895339e-01	114	5.1286439467240055e-02	181	-3.7715267793237528e-02
48	-1.0612974904916984e-01	115	6.1202392116556523e-02	182	3.2584665589150824e-02
49	-3.5113217564966312e-02	116	-6.7580753007337319e-02	183	-2.0737283754424712e-02
50	4.0218359017526559e-02	117	-1.6437971040579487e-02	184	1.3864352749485618e-02
51	7.8361783003269556e-02	118	8.3823412299087741e-02	185	-8.7829054862095680e-03
52	7.3398676062824464e-02	119	-3.1129582248823506e-02	186	2.1524752594113381e-04
53	4.0082784033609056e-02	120	-9.0606281623062307e-02	187	8.0141810052076230e-03
54	-2.2383543408815619e-02	121	9.9165641845843672e-02	188	-2.4354075926243869e-02
55	-8.2296082804443393e-02	122	1.8782838667999648e-02	189	5.4932158991081281e-02
56	-8.4147745310137301e-02	123	-9.3854937791789411e-02	190	-8.6782177238567931e-02
57	-7.5234191684223472e-03	124	4.7611614221696491e-02	191	1.0670313317405239e-01
58	8.7766471759585227e-02	125	4.6554985453885927e-02	192	-1.1472547242235932e-01
59	9.9943486158437109e-02	126	-8.0607535393314583e-02	193	1.2161291209232598e-01
60	2.9076457641035492e-02	127	1.3822186988443654e-03	194	-1.3322042163313333e-01
61	-5.7229534535489082e-02	128	1.0686983339236208e-01	195	1.4082258050588076e-01
62	-9.8004508916357966e-02	129	-1.0156480430924225e-01	196	-1.3267679708926211e-01
63	-7.9824646745027372e-02	130	-1.7945677496148255e-02	197	1.0419594282889154e-01
64	1.3507973015108112e-02	131	1.1344820737049335e-01	198	-6.1699999136031615e-02
65	1.1593905953827086e-01	132	-9.1357858286120752e-02	199	2.2550418599469341e-02
66	7.8734679864611079e-02	133	-6.7060256957023360e-03		

Proof: It suffices to note that, since $g_2[n]$ is lossless

$$g_1[n] * g_2[n] = g_2[n] * g_2[-n] = \delta[n]. \qquad \square$$

Corollary 2: Suppose $g_1[n] = \delta[n]$. Then $q[n]$ is white and has variance

$$\begin{aligned} \mathrm{var}_p q[n] &= E_p\left[|q[n]|^2\right] = \sigma_p^2|\mu|^2 + \sigma_p^2\sigma^2 \\ &= \sigma_p^2 E\left[|F(\omega;n)|^2\right]. \end{aligned} \tag{77}$$

Proof: Since $p[n]$ and $z[n]$ are uncorrelated in Theorem 2

$$\mathrm{var}_p q[n] = \mathrm{var}_p(\mu g_2[n] * p[n]) + \mathrm{var}_p\, z[n]. \tag{78}$$

Furthermore, since $g_2[n]$ is lossless, $p[n]$ and $p[n] * g_2[n]$ have the same spectrum and thus

$$\mathrm{var}_p(\mu g_2[n] * p[n]) = |\mu|^2\sigma_p^2.$$

Applying (23) and (19) we then verify (77). $\square$

Finally, to establish Theorem 1 we need only recognize that $\hat{x}[n]$ can be divided into two uncorrelated components

$$\hat{x}[n] = \hat{x}_1[n] + \hat{x}_2[n]$$

where $\hat{x}_1[n]$ is the component due to $x[n]$ and where $\hat{x}_2[n]$ is due to $w[n]$. Using Theorem 2 and Corollary 1 with $p[n] = x[n]$, $q[n] = \hat{x}_1[n]$, and $f[n;k] = c[n;k]$, we see

$$\hat{x}_1[n] \xrightarrow{\text{m.s.}} \mu_c\, x[n] + z[n]$$

where the white noise $z[n]$ has variance $\mathcal{E}_s\sigma_c^2$. Similarly, using Theorem 2 and Corollary 1 with $p[n] = w[n]$, $q[n] = \hat{x}_2[n]$, and $f[n;k] = b[n;k]$ we get that

$$\mathrm{var}\,\hat{x}_2[n] = \mathcal{N}_0\mathcal{W}_0 E\left[|B(\omega;n)|^2\right]. \qquad \square$$

APPENDIX II
OPTIMIZED PRECODER COEFFICIENTS

Tables I–III show the precoder coefficients that were used to generate the experimental results in Section VI. The (normalized) lengths N' of the precoding filters in the tables are, respectively, 13, 27, and 200. The first two of these were obtained by starting with the minimum-loss binary squence of the corresponding length, and locating the unit-energy sequence corresponding to the nearest local minimum of the loss function when the binary constraint is relaxed. A similar procedure was used to obtain the precoding filter of length 200, except that the initial sequence was a chirp sequence of the same length.

ACKNOWLEDGMENT

The author wishes to thank N. S. Jayant, C.-E. Sundberg, N. Seshadri, J. Kovacevic, M. Sondhi, A. Odlyzko, I. E. Teletar, A. Wyner, and S. Shamai (Shitz), all at AT&T Bell Laboratories, for many helpful discussions, comments, and suggestions regarding this work. He also wishes to thank both anonymous reviewers as well as H. Papadopoulos for their careful reading of the manuscript and thoughtful feedback.

REFERENCES

[1] J. G. Proakis, *Digital Communications*, 2nd ed. New York: McGraw-Hill, 1989.
[2] W. C. Jakes, Ed., *Microwave Mobile Communications*. New York: Wiley, 1974.
[3] G. D. Forney, Jr., "Burst-correcting codes for the classic bursty channel," *IEEE Trans. Commun.*, vol. COM-19, pp. 772–781, Oct. 1971.
[4] A. Wittneben, "An energy- and bandwidth-efficient data transmission system for time-selective fading channels," in *Proc. IEEE GLOBECOM*, 1990.
[5] G. W. Wornell, "Spread-signature CDMA: Efficient multiuser communication in the presence of fading," *IEEE Trans. Inform. Theory*, vol. 41, pp. 1418–1438, Sept. 1995.
[6] L. H. Ozarow, S. Shamai (Shitz), and A. D. Wyner, "Information theoretic considerations for cellular mobile radio," *IEEE Trans. Veh. Technol.*, vol. 43, pp. 359–378, May 1994.
[7] A. V. Oppenheim and R. W. Schafer, *Discrete-Time Signal Processing*. Englewood Cliffs, NJ: Prentice-Hall, 1989.
[8] M. J. E. Golay, "A class of finite binary sequences with alternate autocorrelation values equal to zero," *IEEE Trans. Inform. Theory*, vol. IT-18, no. 3, pp. 449–450, 1972.
[9] ——, "The merit factor of long low-autocorrelation binary sequences," *IEEE Trans. Inform. Theory*, vol. IT-28, no. 3, pp. 543–549, 1982.
[10] E. Biglieri, "Ungerboeck codes do not shape the signal power spectrum," *IEEE Trans. Inform. Theory*, vol. IT-32, pp. 595–596, July 1986.
[11] E. A. Lee and D. G. Messerschmitt, *Digital Communication*, 2nd ed. Boston, MA: Kluwer, 1994.
[12] M. Abramowitz and I. A. Stegun, Eds., *Handbook of Mathematical Functions*. New York: Dover, 1965.
[13] W. C. Y. Lee, "Estimate of channel capacity in Rayleigh fading environment," *IEEE Trans. Veh. Technol.*, vol. 39, pp. 187–189, Aug. 1990.
[14] T. M. Cover and J. A. Thomas, *Elements of Information Theory*. New York: Wiley, 1991.
[15] G. F. M. Beenker, T. A. C. M. Claasen, and P. J. van Gerwen, "Design of smearing filters for data transmission," *IEEE Trans. Commun.*, vol. COM-33, pp. 955–963, Sept. 1985.
[16] K. Popat and K. Zeger, "Robust quantization of memoryless sources using dispersive FIR filters," *IEEE Trans. Commun.*, vol. 40, pp. 1670–1674, Nov. 1992.
[17] C. de Groot, D. Würtz, and K. H. Hoffmann, "Low autocorrelation binary sequences: Exact enumeration and optimization by evolutionary strategies," *Optimization*, vol. 23, pp. 369–384, 1992.
[18] D. V. Sarwate and M. B. Pursley, "Crosscorrelation properties of pseudorandom and related sequences," *Proc. IEEE*, vol. 68, pp. 593–619, May 1980.
[19] D. V. Sarwate, "Mean-square correlation of shift-register sequences," *Proc. Inst. Elec. Eng.*, pt. F, vol. 131, pp. 101–106, Apr. 1984.